COMPARISON OF GROSS AND HISTOPATHOLOGIC FINDINGS WITH QUANTITATIVE COMPUTED TOMOGRAPHIC BONE DENSITY IN THE DISTAL THIRD METACARPAL BONE OF RACEHORSES

MARTHA G. DRUM, CHRISTOPHER E. KAWCAK, ROBERT W. NORRDIN, RICHARD D. PARK, C. WAYNE MCILWRAITH, CLIFFORD M. LES

Comparison of subchondral bone density determined by quantitative computed tomography (CT) with gross and histopathologic changes have not been made in horses. The goal of this study was to determine if mean quantitative CT density and mean voxel standard deviation are associated with the presence and severity of osteochondral lesions in the palmar aspect of the distal third metacarpal bone in racing horses. Metacarpophalangeal joints from nine racehorses were imaged using CT and scored for gross damage. Four-millimeter-thick sagittal and 30° palmar dorsal plane sections were cut, decalcified and stained with hematoxylin and eosin from the distal third metacarpal bone. Microscopic osteochondral lesions and subchondral remodeling were scored on a scale of 0–3. Percent subchondral bone, expressed as the ratio of bone volume to tissue volume, was also measured. Mean quantitative CT density and mean voxel standard deviation were measured from three-dimensional models of CT images comparable with histologic sections. Mean quantitative CT density was not associated with lesion severity or number of lesions. A weak correlation between mean quantitative CT density and gross score was found, but mean quantitative CT density was not predictive for gross score. Mean voxel standard deviation was not correlated with gross or histopathologic measures, but was predictive of mild osteochondral lesions. Results support the association of subchondral remodeling with the development of palmar metacarpal lesions. However, there was not a strong correlation between mean quantitative CT density or mean voxel standard deviation and histopathologic lesions of the distal third metacarpal bone. *Veterinary Radiology & Ultrasound, Vol. 48, No. 6, 2007, pp 518–527.*

Key words: bone density, histology, racehorses, quantitative computed tomography, quantitative computed tomography.

Introduction

MUSCULOSKELETAL INJURY AND disease are responsible for significant morbidity and mortality in racing horses.[1] Overload arthrosis has been suggested as the primary etiology of osteochondral lesions in racehorses.[2] In overload arthrosis, subchondral bone becomes thickened and sclerotic, presumably altering its biomechanics and normal shock absorbing capabilities. Osteochondral lesions in the metacarpophalangeal joint of racehorses can result in condylar fractures and palmar metacarpal bone disease, which includes palmar arthrosis, palmar osteochondral fragmentation, and traumatic osteochondrosis.

Gross and histopathologic characteristics of overload arthrosis in horses have been documented,[3–5] and suggest that subchondral bone plays a role in the development of osteochondral injuries and lesions. Quantitave computed tomograpy (CT) has been used to measure bone mineral density in people[6] and horses.[7] Also, CT osteoabsorptiometry maps have allowed documentation of bone density of articular surface in people[8] and horses.[9] However, no direct comparison of subchondral bone density obtained using quantitative CT and gross or histopathologic changes has been made in horses. A measurable association between quantitative CT density and articular lesions would be useful to noninvasively diagnose joint disease.

The goal of this study was to determine if mean quantitative CT density and mean voxel standard deviation are associated with the presence and severity of gross and histopathologic osteochondral lesions of the distal third metacarpal condyle in racing horses.

Materials and Methods

Metacarpophalangeal joints were collected from nine horses euthanized during the 2003 Colorado racing season. Five horses were euthanized for musculoskeletal injuries

From the Department of Clinical Sciences, Equine Orthopaedic Research Center, (Drum, Kawcak, McIlwraith), the Department of Microbiology, Immunology, and Pathology, (Norrdin), the Department of Environmental and Radiologic Health Sciences, (Park) Colorado State University, Fort Collins, CO 80523, and the Bone and Joint Center, Henry Ford Hospital, Detroit, MI 48202 (Les).

Address correspondence and reprint requests to Martha G. Drum, at the above address. E-mail: mdrum@utk.edu

Received January 29, 2007; accepted for publication May 21, 2007.
doi: 10.1111/j.1740-8261.2007.00289.x

(sesamoid fracture, carpal bone fracture, scapular fracture, proximal interphalangeal joint luxation, and proximal phalanx fracture), two horses were euthanized for respiratory disease, one horse was euthanized for gastrointestinal disease, and one horse was euthanized for acute collapse. Routine necropsy examinations were performed on the horses after the metacarpophalangeal joints were harvested.

CT imaging was performed on a Picker PQ CT* at 140 kVP with a slice thickness of 1.5 mm, 180 mm field of view, and a 512×512 voxel matrix, which creates a 0.4 mm in-plane spatial resolution. CT studies were exported for analysis to the customized image analysis program OsteoApp† that was designed using the Interactive Design Language.‡ Additionally, a tri-calcium phosphate (TCP) density phantom§ was scanned at the end of each metacarpophalangeal joint scan to convert quantitative CT density measurements from Hounsfield Units to mg/ml TCP using linear regression. Owing to the large size of the phantom, it was not possible to scan both the metacarpophalangeal joint and the phantom in the same field unless scan settings were changed.

Metacarpophalangeal joints were disarticulated after CT scanning and scored for superficial palmar gross pathologic changes on a scale of 0–4 (Fig. 1 and Table 1). After assigning a gross score, the entire metacarpophalangeal joint was photographed for reference. The distal third metacarpal bone was removed with a band saw approximately 3 cm proximal to the medial condylar surface, and the dissected distal third metacarpal bone was photographed for reference. The condyles were wrapped in physiologic-buffered saline-soaked gauze and frozen at -20°C for storage until further processing.

Each distal third metacarpal bone was further cut precisely at 2 cm proximal to the medial condyle, which was measured along the central axis of rotation. Next, sagittal and palmar dorsal plane sections were obtained, respectively, using a precision cutting system¶ in 4-mm-thick sections. The palmar dorsal plane sections were cut using a specialized jig such that the dorsal plane section was taken 30° palmar to the central axis of rotation (Fig. 2A). The sections were then fixed in 10% buffered formalin for 72 h. Samples were rinsed with tap water and placed in ethylenediaminetetraacetic acid (EDTA) decalcifying solution‖ at a volume of 10:1 for 3 weeks. Although the EDTA solution was changed every 2–3 days to accelerate decalcifying, the samples were too hard for histologic processing as determined by using a #10 scalpel blade to make test cuts on the proximal edge of the samples. Samples were rinsed in tap water, radiographed, and placed in 10% formic acid with polyacrimide resin beads (Amberlite IR-120 [plus] ion-exchange resin, sodium form# to further decalcify the samples. Based on repeat radiographs, decalcification was complete in 2 days. Additionally, the samples were tested and found to be free of calcium using an aluminum hydroxide decalcification end point assay.** Samples were then embedded in paraffin and sectioned for staining with hematoxylin and eosin (H&E).

Osteochondral lesions apparent on H&E sections were graded for severity on a scale of 0–4 (Fig. 3 and Table 2). Subchondral remodeling at the chondro-osseous interface was scored on a scale of 0–3 (Fig. 4). Percent subchondral bone volume was measured using a software package‡‡ that measured subchondral bone area as a percent of total tissue area. Because horses could potentially have multiple lesions within the same limb, the additional variables of lesion severity and number of lesions per section were created. Lesion severity was calculated by adding the individual lesion scores to create an overall score for each histologic section.

CT images were imported to a PC workstation for three-dimensional modeling using OsteoApp.† CT images were cropped to 4-mm-thick sections in the dorsal plane 30° palmar to the central axis of rotation or at specific sites in the sagittal plane in accordance with histologic sections (Fig. 2A). Voxel thresholding at 500 Hounsfield units was used to create a three-dimensional volume of the cropped section (Fig. 2B). A region of interest was drawn by physically measuring the size of the histologic section and creating the same size area as the histologic section (Fig. 2C). Mean quantitative CT density and mean voxel standard deviation values were recorded in Hounsfield Units and converted to mg/ml TCP. Mean voxel standard deviation was used as a measure of variability of density within the measured region of interest.

Probability plots for lesion severity, number of lesions, mean quantitative CT density, mean voxel standard deviation, gross score, and age were examined for normality. A logarithmic transformation of age was used for analysis as the logarithmic regression of age vs. mean quantitative CT density was a better fit ($r^2 = 0.36$) than the linear regression of age vs. mean quantitative CT density ($r^2 = 0.25$). Pearson's correlation coefficients were calculated for mean quantitative CT density, mean voxel standard deviation, age, subchondral remodeling score, subchondral bone tissue to total tissue ratio, number of lesions, lesion severity score, and gross score for each histologic plane (sagittal or dorsal) and pooled data for both section planes. Terms

*Philips Medical, Barthow, WA.
†Colorado State University, Fort Collins, CO.
‡Research Systems Inc., Boulder, CO.
§Computerized Image Reference Systems Inc., Fairfax, VA.
¶Exakt Trennschleifsystem, Exakt-Apparatebau, Norderstedt, Germany.
‖Richard-Allan Scientific Decalcifying Solution, Kalamazoo, MI.
#Sigma-Aldrich Inc., St. Louis, MO.
**Diagnostic Laboratory Colorado State University, Fort Collins, CO.
‡‡ImagePro, Media Cybernetics, Silver Spring, GA.

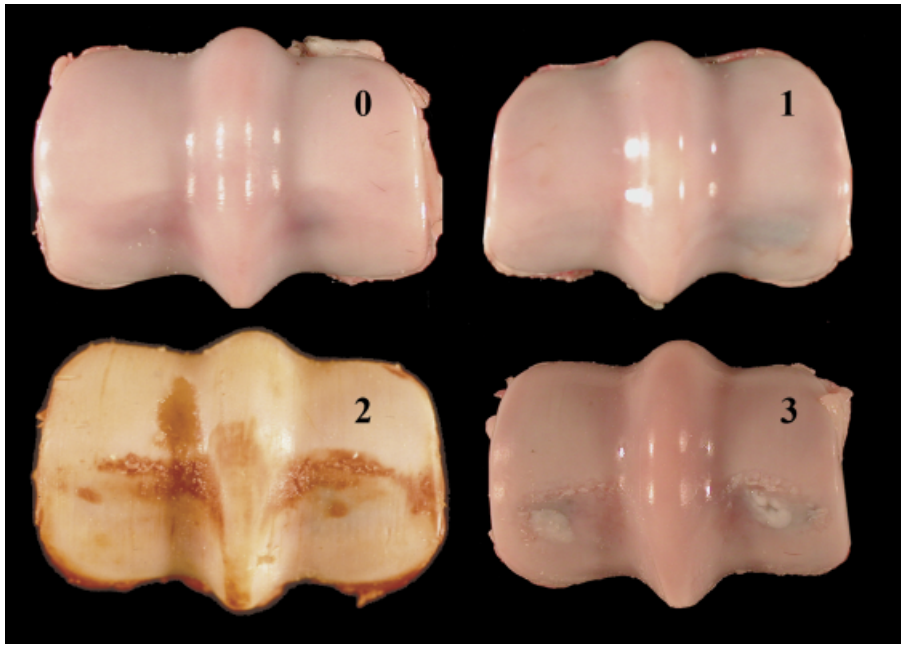

FIG. 1. Examples of superficial gross palmar scores. Refer to Table 1 for full description of each grade.

were considered significant at $P<0.05$, and a data trend was considered at $\alpha<0.10$.

A mixed model analysis was performed with a backwards selection method ($\alpha<0.10$) for gross score, lesion severity and number of lesions as response variables. Subchondral remodeling score, mean quantitative CT density, mean voxel standard deviation, section, limb, and age were fixed model terms, and horse was the random term in the model. Pairwise comparisons for significant categorical predictors were performed using Fisher's least significant differences. Subchondral remodeling score was also analyzed using a backward elimination method with mean quantitative CT density, mean voxel standard deviation, section, limb, and age as predictors. Additionally, a logistic regression for each lesion grade was modeled with a backwards selection method ($\alpha=0.10$) for mean quantitative CT density, mean voxel standard deviation, and age.

TABLE 1. Description of Superficial Palmar Gross Scoring Scheme

Gross Score	Description
0	No visible abnormalities or changes in cartilage or bone.
1	Minimal scoring with fibrillation of cartilage.
2	Mild erosion, small pits and/or more prominent fibrillation
3	Similar changes as in grade 2, but additionally focal divots or indentations of cartilage with/without focal cartilage opacities, and partial to full-thickness erosions in small (4–8 mm) areas.
4	Extensive degeneration, erosion, and ulceration of cartilage with some exposure and/or loss of underlying bone, generally involving a large (1 cm or greater) area. Note: No grade 4 lesions were observed.

Results

There were three females and six males, of which there were two Quarter Horses (one male, one female) and seven Thoroughbreds (two females, five males). They ranged in age from 43 to 138 months with a mean ($\pm$ standard deviation) age of 66.7 $\pm$ 38.2 months and a median age of 43 months.

Nine grade 1 gross pathologic lesions were observed. Six of the grade 1 lesions were bilateral in a female Thoroughbred, male Quarter Horse, and a male Thoroughbred. Two of the grade 1 lesions were in left limbs of a female Quarter Horse and a male Thoroughbred, and one of the grade 1 lesions was in the right limb of a male Thoroughbred. One grade 2 gross pathologic lesion was observed in the right limb of a male Thoroughbred. Four grade 3 gross pathologic lesions were observed (one male Thoroughbred with bilateral lesions, two male Thoroughbreds with left limb lesions). No grade 4 gross pathologic lesions were observed. The remaining samples had no observable lesions.

A total of seven grade 1 histopathologic lesions, six grade 2 histopathologic lesions, and one grade 3 histopathologic lesion were identified. No grade 4 histopathologic lesions were observed in any section. Table 3 summarizes the distribution of the observed histopathologic lesions by limb for each section. Three horses had more than one lesion in a single section. One horse had a grade 2 lesion in the medial condyle and a grade 3 lesion in the in the lateral condyle of a right dorsal section. Another horse had a right limb sagittal section with a grade 1 lesion adjacent to the transverse ridge and a grade 2 lesion in the

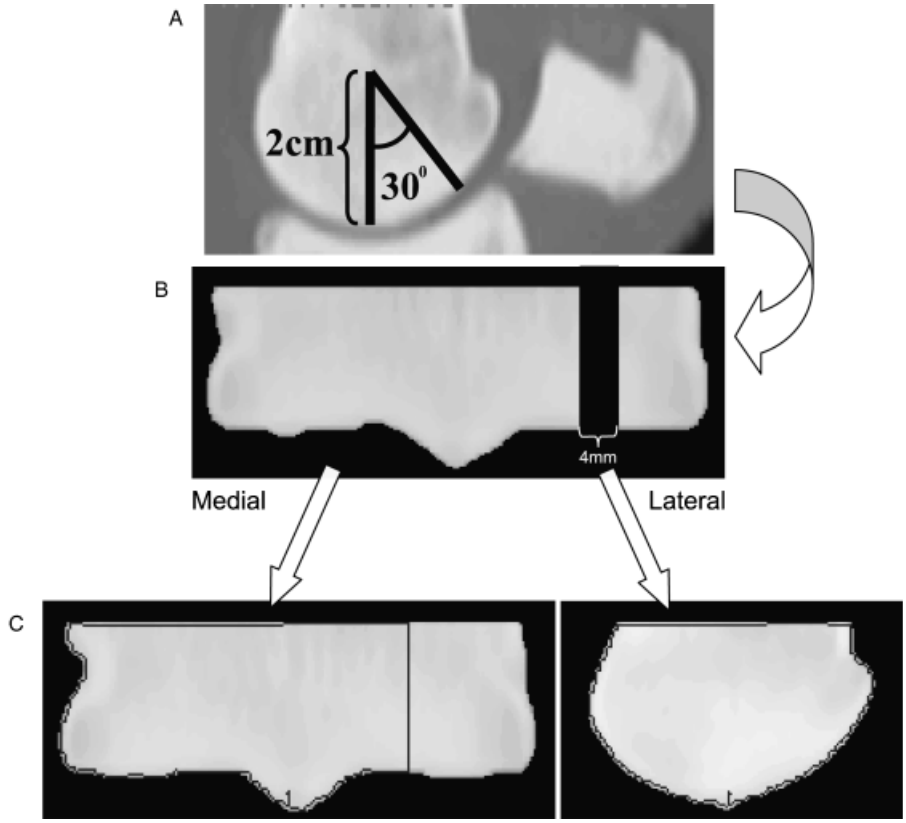

FIG. 2. Flowchart of slice rendering. (A) Measurement techniques to create a 30° palmar 4-mm-thick section. (B) 3D representation of a palmar slice with sagittal slice previously removed as was done in cutting histologic sections. (C) Palmar and sagittal slices with ROIs drawn over areas of interest in accordance with histologic sections.

palmar aspect of the condyle. The third horse had two grade 1 histopathologic lesions in the medial condyle from a left limb dorsal section. Mean, standard deviation and standard error of the mean for each response variable is listed in Table 4 by section. The remaining samples had no observable lesions.

Probability plots were acceptable, that is plots appeared linear, for all parameters except lesion severity. A square-

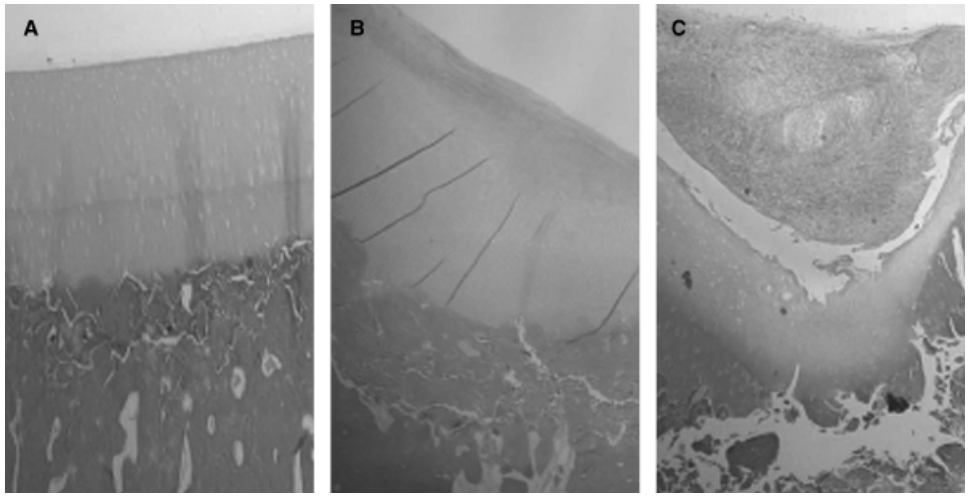

FIG. 3. Grades 1–3 osteochondral lesion appearance on hematoxylin and eosin (H&E) staining. (A) Grade 1 lesion, (B) grade 2 lesion, and (C) grade 3 lesion. Please refer to Table 3 for complete description of each lesion grade.

TABLE 2. Description of Microscopic Features in Osteochondral Lesion Grading Scheme

0	No visible changes in cartilage or bone
1	Minor disruption of subchondral bone matrix. Lesion occupies <25% of histologic condylar surface, and extends no more than 1–2 mm deep to the normal chondrosseous junction. Some of the matrix within the lesion is pale staining and occasional marrow spaces contain debris. Tidemark is reduplicated. Fibrin may be present in the subchondral bone layer. No apparent superficial cartilage fibrillation.
2	More severe disruption of subchondral bone matrix. Areas of matrix are fragmented to comminuted. Lesion occupies 25–50% of histologic condylar surface and extends approximately 2–4 mm deep to the normal osteochondral junction. A significant amount of the subchondral bone matrix is pale staining, and there is significant debris within marrow spaces. The tidemark is reduplicated and often disrupted. Moderate amounts of fibrin present in the subchondral bone layer. Cartilage overlying lesion is thickened with superficial cartilage erosion and fibrillation. Reparative fibrocartilage is also apparent in the superficial cartilage layers.
3	Complete collapse of osteochondral tissue. Lesion occupies >50% of histologic condylar surface and extends >3 mm deep to the normal osteochondral junction. Pale staining subchondral bone matrix and fibrin are abundant. The tidemark is reduplicated and often disrupted. Superficial thickening of cartilage and/or fibrocartilage present and may be completely detached from thickened deeper cartilage.
4	Obvious loss of osteochondral tissue leaving an ulcer (not observed).

root transformation was performed for lesion severity to normalize values for split–split plot analysis.

Mean quantitative CT density correlated well with the subchondral bone tissue to total tissue ratio (Fig. 5) for pooled ($r=0.84$, $P<0.001$), dorsal ($r=0.90$, $P<0.0001$), and sagittal ($r=0.80$, $P=0.001$) images. Weak, but significant correlations were found between mean quantitative CT density and severity of subchondral remodeling score ($r=0.38$, $P=0.04$) and gross score ($r=0.36$, $P=0.04$) for pooled slice data. A trend in correlations of mean quantitative CT density and lesion severity of pooled slices ($r=0.34$, $P=0.07$), and mean quantitative CT density and gross score of dorsal slices ($r=0.36$, $P=0.05$) was observed. Age was significantly correlated with both number of lesions ($r=0.52$, $P=0.03$) and lesion severity ($r=0.50$, $P=0.04$) in sagittal sections. In pooled slices, age was significantly correlated with gross score ($r=0.43$, $P=0.02$). This relationship was not found when only sagittal slices were considered ($r=0.39$, $P=0.13$) and only a data trend existed in palmar dorsal plane slices ($r=0.49$, 0.09).

Mean voxel standard deviation did not correlate with any parameters ($P>0.10$). Number of lesions correlated significantly with subchondral remodeling score for pooled ($r=0.51$, $P=0.0036$) and sagittal ($r=0.63$, $P=0.0007$) images but not for dorsal images ($r=0.47$, $P=0.11$). Lesion severity correlations with severity of subchondral remodeling score correlated well for all slices ($r=0.62$, $P=0.0003$ pooled, $r=0.63$, $P=0.02$ dorsal, $r=0.69$, $P=0.002$ sagittal). Finally, gross score and subchondral remodeling score were highly correlated in dorsal slices ($r=0.82$, $P=0.0005$), and marginally correlated to pooled slices ($r=0.47$, $P=0.008$). However, there was no correlation with subchondral remodeling and gross score in sagittal slices ($r=0.22$, $P=0.39$).

An interesting lesion of osteochondral tissues, including subchondral bone and calcified cartilage layer, was observed during histologic grading of the samples (Fig. 6). The calcified cartilage and subchondral bone contained vertically oriented splits that were only visible in the palmar dorsal plane sections. These splits appeared to range in severity from mild to severe and were localized to the condylar groove. Although splitting of the calcified cartilage matrix can be attributed to artifact during histologic sectioning, the vertically oriented splits seen in this study were thought to be actual representations of matrix defects because debris and fibrin were visible within the splits. Also, because the splits were localized to the condylar groove,

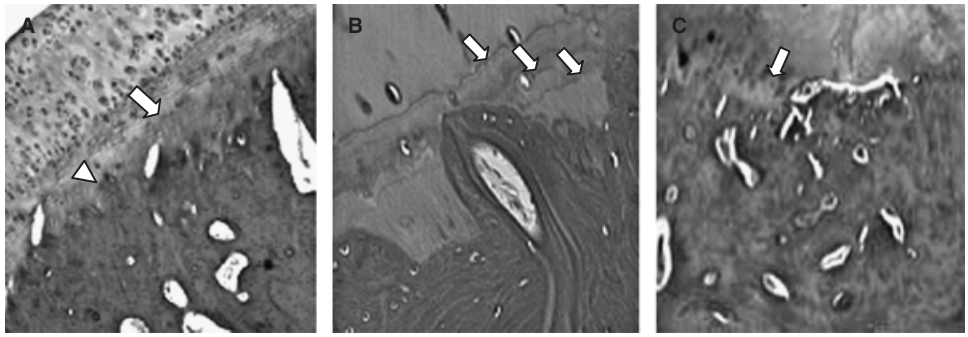

FIG. 4. Severity of subchondral remodeling from 1 to 3. (A) Grade 1 severity of subchondral remodeling is advancement of the subchondral bone into the calcified cartilage layer with scalloped subchondral bone margins (arrowheads), but not crossing any tidemarks (block arrow). (B) Grade 2 severity of subchondral remodeling is subchondral bone advancement through the calcified cartilage layer, crossing one or more tidemarks, but below the most superficial tidemark front. Tidemark fronts are identified by block arrows. (C) Grade 3 severity of subchondral remodeling is subchondral bone advancement through the calcified cartilage layer and disruption of the tidemark front (block arrow).

TABLE 3. Lesion Distribution by Section

	Bilateral Lesions	Unilateral Lesions	Left Limbs	Right Limbs	Total Lesions
Sagittal					
Grade 1	1	2	1	4	5
Grade 2	1	1	1	2	3
Grade 3	0	0	0	0	0
Dorsal					
Grade 1	0	2	2	0	2
Grade 2	1	1	1	2	3
Grade 3	0	1	0	1	1
TOTAL	3	7	5	8	13

this may be why the splits were seen only in palmar dorsal plane sections as sagittal plane sections were not taken from this region.

Subchondral bone tissue to total tissue ratio only correlated significantly with sagittal slice gross score ($r = 0.61$, $P = 0.01$) in addition to the previously mentioned mean quantitative CT density correlations. Trends existed with correlations of subchondral bone tissue to total tissue ratio and sagittal slice lesion severity ($r = 0.51$, $P = 0.03$), and pooled slice gross score ($r = 0.36$, $P = 0.05$). A trend was observed between gross score and lesion severity for dorsal slices ($r = 0.53$, $P = 0.06$), but correlations were not significant between gross score and lesion severity in sagittal or pooled slices ($P > 0.10$).

Left limbs had significantly higher gross scores than right limbs ($P = 0.03$). A trend existed for the association between gross score and mean voxel standard deviation ($P = 0.08$), and no model term interactions were significant. Severity of subchondral remodeling significantly predicted subchondral bone tissue to total tissue ratio ($P = 0.04$), but no other terms were significant in the mixed-model regression analysis.

Lesion severity was only predicted significantly by subchondral remodeling score ($P = 0.003$, Fig. 7). Grade 2 severity of subchondral remodeling had significantly higher lesion severity scores than grades 0 and 1 severity of subchondral remodeling ($P < 0.02$). Grade 3 severity of subchondral remodeling had significantly higher lesion severity scores than grades 0 and 1 severity of subchondral remodeling ($P < 0.001$) but not grade 2 severity of subchondral remodeling ($P = 0.13$). Lesion severity of grade 1 severity of subchondral remodeling was not significantly different than grade 0 severity of subchondral remodeling ($P = 0.82$). Number of lesions were also predicted significantly by subchondral remodeling score ($P = 0.008$) in the mixed-model regression, but age was a trend in association ($P = 0.05$, Fig. 8). The interaction of age and subchondral remodeling score was not significant ($P = 0.18$). In contrast to lesion severity scores, grade 2 severity of subchondral remodeling had significantly higher number of lesions that grade 1 ($P = 0.03$) but not grade 0 ($P = 0.3$). Grade 3 severity of subchondral remodeling had significantly higher

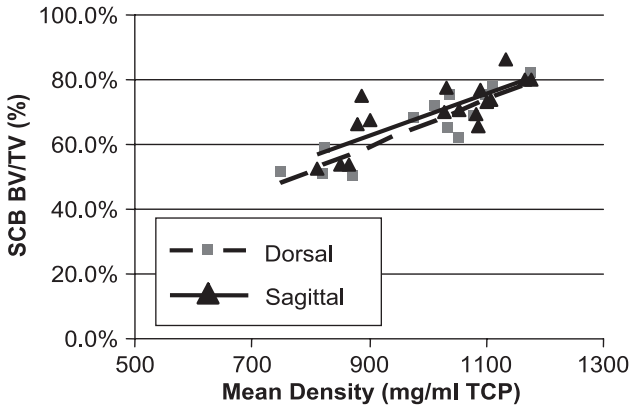

FIG. 5. Mean quantitative CT density vs. subchondral bone tissue to total tissue ratio with linear regression lines for each histologic plane (dorsal or sagittal). Each section correlated well with mean quantitative CT density ($r = 0.90$ dorsal, $r = 0.80$ sagittal).

TABLE 4. Mean, Standard Deviation and Standard Error of the Mean for each Response Variable by Section

Section	*N*	Variable	Mean	SD	SEM
Dorsal	13	Mean (TCP)	986	131	36.5
		MVSD (TCP)	144	21.4	5.94
		Lesion Score	0.923	1.50	0.415
		Number of Lesions	0.538	0.776	0.215
		Gross Score	1.23	1.17	0.323
		SC BV/TV	70.8	12.4	3.43
		SCR	0.692	0.947	0.263
Sagittal	17	Mean (TCP)	1010	119	28.9
		MVSD (TCP)	131	19.2	4.66
		Lesion Score	0.647	0.931	0.226
		Number of Lesions	0.471	0.624	0.151
		Gross Score	1.29	1.10	0.268
		SC BV/TV	57.4	14.2	3.46
		SCR	1.24	0.970	0.235

SD, standard deviation; SEM, Standard error of the mean; TRP, Tri-calcium phosphate; MVSD, Mean voxel standard deviation; SC BV/TV, Subchondral bone volume/tissue volume; SCR, Subcondral remodeling score.

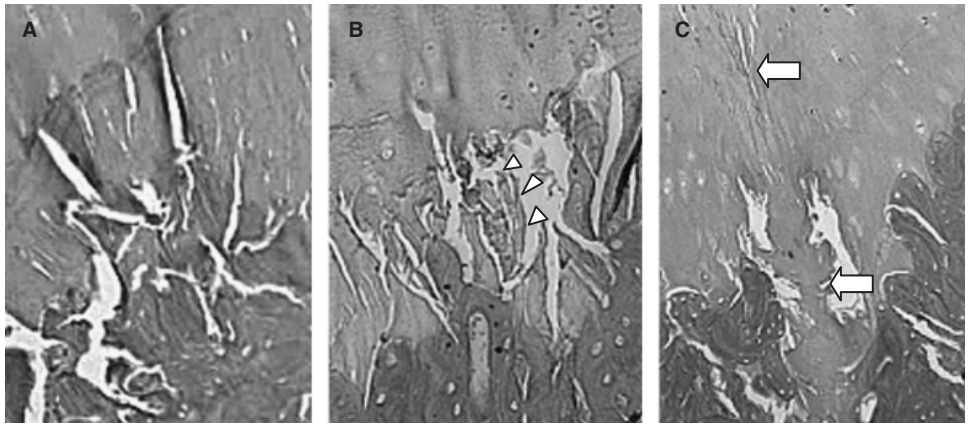

FIG. 6. Severity of osteochondral splitting from mild to severe. (A) Mild splits involve the tidemark and subchondral bone, but are simple linear defects. (B) Moderate splits have fragments and debris (arrowheads) within the split and connections between splits. (C) Severe splits involve articular cartilage and displacement of calcified cartilage fragments into the underlying subchondral bone (block arrows).

number of lesions than grade 0 and 1 ($P<0.01$) but not grade 2 lesions ($P=0.13$).

There was a negative trend in probability of having a grade 1 lesion for mean voxel standard deviation ($P=0.05$). The odds ratio for mean voxel standard deviation and grade 1 lesions was OR = 0.951 [confidence interval (CI): 0.905–0.998]. However, no terms were significant for grades 2 or 3 lesions.

Discussion

Although no direct comparisons of CT density and histologic measures or observations have been done in horses, previous studies in humans, mice, and dogs have found good to excellent correlations of CT density with cortical porosity[10,11] and amount of mineralized matrix[12,13]. Furthermore, there has been no published work to date correlating quantitative CT density with subchondral bone density.

Mean quantitative CT density predicted and correlated well with subchondral bone tissue to total tissue ratio. This relationship is somewhat intuitive because both are measures of density. Alternatively, mean quantitative CT density was not a good predictor of lesion severity or number of lesions in a mixed-model regression, nor was there a good correlation between mean quantitative CT density and lesion severity or number of lesions. A weak correlation between mean quantitative CT density and gross score existed, but mean quantitative CT density was not associated with gross score when analyzed in a mixed-model regression. The small sample size and subsequently limited number of lesions could have reduced the power of this study and obscured true associations (or lack thereof). Another possible reason for the weak relationship of mean

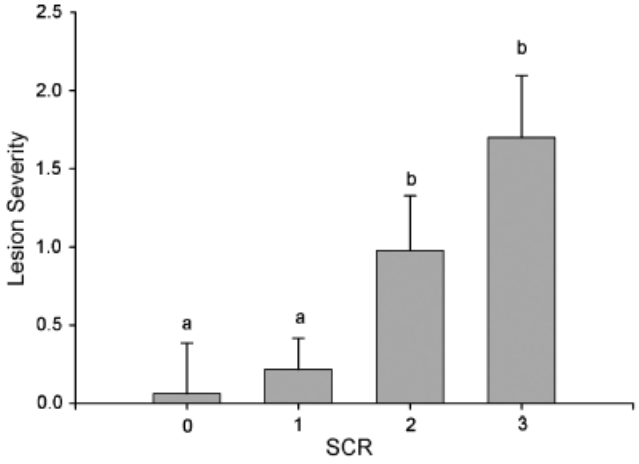

FIG. 7. Severity of lesions for each subchondral remodeling score. Different letters indicate significant differences at $P<0.05$.

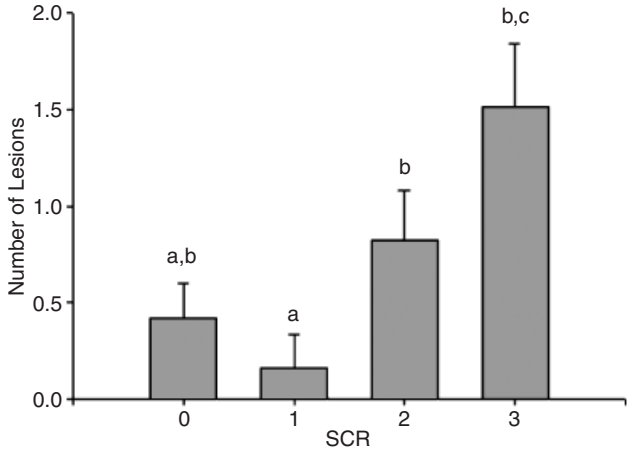

FIG. 8. Number of lesions for each subchondral remodeling score (SCR) adjusted for age. Different letters indicate significant differences at $P<0.05$.

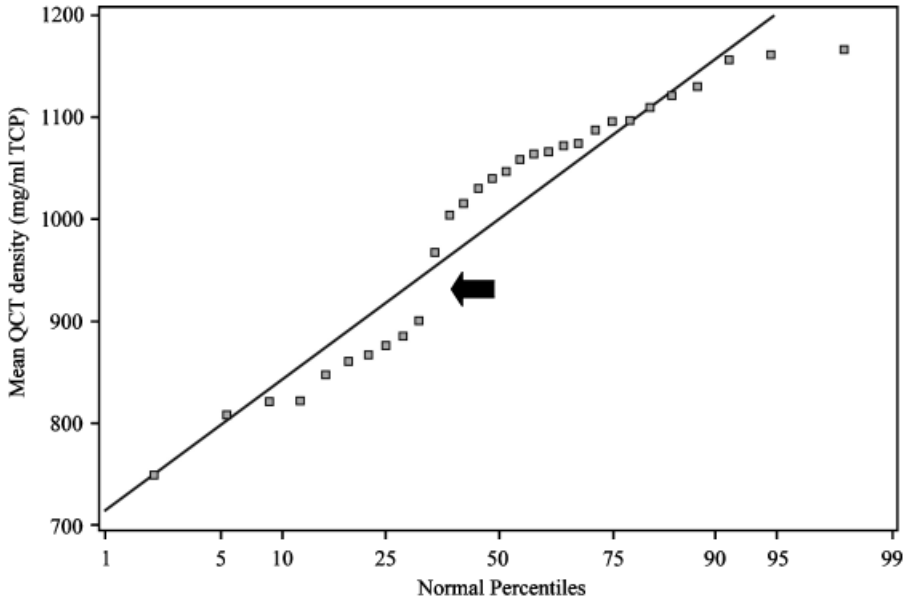

FIG. 9. Probability plot of mean quantitative CT density. The gap (arrow) in mean quantitative CT density points indicates there is one group of samples with high-density values and one group of samples with low-density values. This likely represents two separate populations of horses, each with different mean quantitative CT density values.

quantitative CT density and gross pathologic score is that there may be a biphasic distribution of osteochondral lesions in racehorses, as is suggested by the break in distribution of the mean quantitative CT density probability plots (Fig. 9). In that scenario, the correlation would be weakened because one would be trying to make a single correlation for two different populations with two different variations. While mean quantitative CT density was not associated with histologic lesions, it was mildly correlated with subchondral remodeling score indicating that increased density may be indirectly associated with lesion pathology.

Although mean voxel standard deviation was associated with grade 1 lesions in a mixed-model regression, the associated risk was slight. The negative probability of mean voxel standard deviation with grade 1 lesions suggests that as bone density becomes more homogenous (decreased mean voxel standard deviation), the 5% increase in grade 1 histopathologic subchondral lesions. In horses exercised for 6 months on a high-speed treadmill, there was a loss of incongruity in the metacarpophalangeal joint. The treadmill exercised horses had a homogenization of subchondral bone density across the distal third metacarpal condyle due to a significantly higher percentage of highly dense bone occupying the surface of the distal metacarpal condyle compared with hand-walked horses.[9] Also, palmar arthoses occurred more frequently in exercised horses.[9] as well as an increase of microdamage index.[2] Thus, osteochondral damage was associated with horses in which a specific range of subchondral bone density dominated. This is compatible with the findings in this study that a decreased mean voxel standard deviation is associated with development of osteochondral lesions. However, the odds ratio did not indicate a substantial increased risk with decreased mean voxel standard deviation in this study. Again, given the small number of total lesions and that the observed lesions were relatively mild, this relationship is tenuous at best. Additionally, mean voxel standard deviation may play a different role as a predictor of osteochondral damage over a large surface area of bone in comparison with the deeper, single sections of bone used in this study, and larger studies with more power are warranted to determine what role mean voxel standard deviation plays in predicting osteochondral damage in the equine distal third metacarpal bone.

The vertical cracks observed using H&E sections has not been reported in horses, but the vertical splitting of calcified cartilage and subchondral bone has been observed in horses previously.[14] In that study, cracks (splits) were observed in the subchondral bone and calcified cartilage of the third metacarpal condyle. The cracks were visualized in the parasagittal groove using microradiography and scanning electron microscopy, and were significantly more severe than the cracks observed in this study. In another study of macroscopic pathologic lesions of equine distal third metacarpal bones,[15] vertical cracks were found in the calcified cartilage and subchondral bone were associated with fracture lines in the palmar condylar groove of the distal third metacarpal bone. Splitting of the calcified cartilage layer has also been observed using routine histology

in spontaneous osteoarthritis of hamsters, but splits were of a horizontal orientation in the plane of the tidemark.[16] Density gradients between the sagittal ridge and condylar surface have been reported,[17] as well as osteoporosis of bone adjacent to the condylar groove from post-mortem studies of condylar fractures.[18] Thus, osteochondral splitting may play a significant role in the development of fractures in racehorses and a further study to determine how vertically oriented osteochondral splits are associated with condylar fractures is warranted.

The presence of a bimodal distribution, represented by a gap in data points of the mean quantitative CT density normality plots, suggest there are actually two populations in this study, one group of high density and one group of low density. One possible explanation is that the lower density group could be undergoing intense bony remodeling, which could reduce bone density. This would occur if the rate of turnover is faster than the rate of mineralization of new bone matrix. Another factor which could contribute to the lower bone density is the bony modeling that occurs in young, growing horses, which would increase the amount of lower density bone in comparison with skeletally mature horses. Currently, there is no published research linking a lower density, poor quality bone with condylar fractures of racehorses, but condylar fractures have been thought to occur in young, training racehorses.[5] Conversely, the group of higher densities may relate more to the changes seen in overload arthrosis and palmar metacarpal bone disease of older highly trained racehorses.[5] We cannot determine if condylar fractures and palmar metacarpal bone disease are related to the bimodal distribution seen in mean quantitative CT density in this study, but it does warrant further investigation to determine if the bimodal distribution of density occurs in a larger population of racehorses with condylar fractures and palmar metacarpal bone disease.

The present study supported the hypothesis that subchondral remodeling plays a significant role in the development of palmar osteochondral lesions in racing horses. There were good correlations of subchondral remodeling score with the number of lesions and lesion severity. Subchondral remodeling score was also significantly associated with lesion severity and number of lesions in a mixed-model regression. Limb differences in gross pathologic score suggest that left limbs are more susceptible to gross damage than right limbs. This in agreement with reports that condylar fractures and catastrophic injuries are more common in the left limbs of racing horses[1,19,20].

The subchondral remodeling scoring system developed for this study proved useful and predictive of microscopic osteochondral lesions although is was not predictive of gross pathologic change in racing horses. Similar differences in the severity of subchondral remodeling in pathologic distal third metacarpal condyles have been described,[17] but no direct comparisons were made with lesion outcome. Thus, amount of subchondral remodeling should be considered in future histopathologic studies to further understand in the pathogenesis and determine predictability of these lesions.

In conclusion, mean quantitative CT density was not associated with osteochondral lesions typical of racing horses in this study. Mean voxel standard deviation had a slight association with mild osteochondral lesions in racing horses, and should be investigated in future studies as a potential predictor of osteochondral damage. Increased subchondral remodeling was observed in osteochondral lesions of racing horses and the histopathologic scoring system used in this study was a good measure of microscopic osteochondral lesion severity in racing horses.

ACKNOWLEDGMENTS

The authors would like to thank the Colorado State University Research Council for funding this research, and the Colorado Racing Commission for their cooperation. A portion of this research was presented at the 52nd annual meeting of the Orthopaedic Research Society.

REFERENCES

1. Estberg L, Stover SM, Gardner IA, et al. Fatal musculoskeletal injuries incurred during racing and training in thoroughbreds. J Am Vet Med Assoc 1996;208:92–96.

2. Norrdin RW, Kawcak CE, Capwell BA, McIlwraith CW. Subchondral bone failure in an equine model of overload arthrosis. Bone 1998;22:133–139.

3. Pool RR. Joint disease in the athletic horse. Proc Am Assoc Eq Pract 1995;41:20–34.

4. Pool RR, Meagher DM. Pathologic findings and pathogenesis of racetrack injuries. Vet Clin North Am Equine Pract 1990;6:1–30.

5. Hornof WJ, O'Brien TR, Pool RR. Osteochondritis dissecans of the distal metacarpus in the adult racing thoroughbred horse. Vet Radiol Ultrasound 1981;22:98–102.

6. Cann CE. Quantitative CT for determination of bone mineral density: a review. Radiology 1988;166:509–522.

7. Firth EC, Rogers CW, Doube M, Jopson NB. Musculoskeletal responses of 2-year-old Thoroughbred horses to early training. 6. Bone parameters in the third metacarpal and third metatarsal bones. NZ Vet J 2005;53:101–112.

8. Muller-Gerbl M. The subchondral bone plate. Adv Anat Embryol Cell Biol 1998;141:1–134.

9. Kawcak CE, McIlwraith CW, Norrdin RW, Park R.D, Steyn PS. Clinical effects of exercise on subchondral bone of carpal and metacarpophalangeal joints in horses. Am J Vet Res 2000;61:1252–1258.

10. Markel MD, Morin RL, Wikenheiser MA, Lewallen DG, Chao EY. Quantitative CT for the evaluation of bone healing. Calcif Tissue Int 1991;49:427–432.

11. Wachter NJ, Krischak GD, Mentzel M, et al. Correlation of bone mineral density with strength and microstructural parameters of cortical bone in vitro. Bone 2002;31:90–95.

12. Mankani MH, Kuznetsov SA, Avila NA, Kingman A, Robey PG. Bone formation in transplants of human bone marrow stromal cells and hydroxyapatite-tricalcium phosphate: prediction with quantitative CT in mice. Radiology 2004;230:369–376.

13. Boyde A, Haroon Y, Jones SJ, Riggs CM. Three dimensional structure of the distal condyles of the third metacarpal bone of the horse. Equine Vet J 1999;31:116–120.

14. Riggs CM, Whitehouse GH, Boyde A. Pathology of the distal condyles of the third metacarpal and third metatarsal bones of the horse. Equine Vet J 1999;31:140–148.

15. Radtke CL, Danova NA, Scollay MC, et al. Macroscopic changes in the distal ends of the third metacarpal and metatarsal bones of Thoroughbred racehorses with condylar fractures. Am J Vet Res 2003; 64:1110–1116.

16. Otterness IG, Chang M, Burkhardt JE, Sweeney FJ, Milici AJ. Histology and tissue chemistry of tidemark separation in hamsters. Vet Pathol 1999;36:138–145.

17. Riggs CM. Aetiopathogenesis of parasagittal fractures of the distal condyles of the third metacarpal and third metatarsal bones—review of the literature. Equine Vet J 1999;31:116–120.

18. Stover SM, Read DH, Johnson BJ, et al. Lateral condylar fracture histomorphology in racehorses. Proc Am Assoc Equine Pract 1994;40: 173.

19. Rick MC, O'Brien TR, Pool RR, Meagher D. Condylar fractures of the third metacarpal bone and third metatarsal bone in 75 horses: radiographic features, treatments, and outcome. J Am Vet Med Assoc 1983;183:287–296.

20. Bassage LH, Richardson DW. Longitudinal fractures of the condyles of the third metacarpal and metatarsal bones in racehorses: 224 cases (1986–1995). J Am Vet Med Assoc 1998;212:1757–1764.